Heliyon 10 (2024) e34397

Contents lists available at ScienceDirect

Heliyon

journal homepage: www.cell.com/heliyon

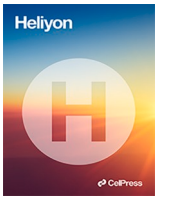

Research article

AP-1 inhibitor induces ferroptosis via the PI3K/AKT pathway in multiple myeloma cells

Sishi Tang [a], Jing Liu [a], Fangfang Li [a], Yuhan Yan [a], Xinyi Long [a], Yunfeng Fu [b,*]

[a] Department of Hematology, The Third Xiangya Hospital, Central South University, Changsha 410013, China
[b] Department of Blood Transfusion, The Third Xiangya Hospital, Central South University, Changsha 410013, China

ARTICLE INFO

Keywords:
T-5224
Ferroptosis
PI3K/AKT
Multiple myeloma
Bortezomib

ABSTRACT

Multiple myeloma (MM) is an incurable malignancy of plasma cells that is sensitive to T-5224, an AP-1 inhibitor. Previous study indicated that T-5224 inhibits proliferation and induces apoptosis in MM cells. However, the high mortality cannot be fully explained. To date, no studies have investigated ferroptosis induced by T-5224 in MM. Therefore, we further investigated the mechanism by which T-5224 kills MM cells. We observed that T-5224 exhibits antimyeloma properties both in vitro and in vivo. T-5224-induced MM cell death was reversed by the ferroptosis-specific inhibitor ferropstatin-1 (Fer-1). The protein levels of the key ferroptosis regulators GPX4 and SLC7A11 were decreased by T-5224 in MM cells. Furthermore, T-5224 reduced the phosphorylation of PI3K and AKT signaling pathway components, ultimately causing MM cell death. Using 740 Y–P, a PI3K activator, and Fer-1, a ferroptosis inhibitor, we discovered that T-5224 induces ferroptosis through the PI3K/AKT pathway. Bortezomib (BTZ), an FDA-approved drug for MM treatment, can be administered in combination with other agents. We evaluated the synergistic effect of BTZ combined with AP-1 inhibitors on MM in vivo. Our findings provide a better theoretical basis for the potential mechanism of T-5224 and a new perspective on MM treatment.

1. Introduction

Multiple myeloma (MM) is a currently incurable malignancy of plasma cells and accounts for 10 % of all hematological malignancies [1,2]. Even newly-developed drugs, including immunomodulatory drugs (e.g., lenalidomide), proteasome inhibitors (e.g., bortezomib), and autologous stem cell transplantation (ASCT), have dramatically improved the prognosis of MM patients. Nonetheless, relapse is inevitable, and some patients will eventually die from treatment-related complications, thus making MM an incurable cancer [3–5]. T-5224, a newly developed selective activator protein-1 (AP-1) inhibitor, is currently being investigated in phase II human clinical trials for arthritis treatment [6]. Furthermore, the anti-inflammatory and anticancer properties of this substance have received increasing amounts of attention [7–9]. The effects of T-5224 are closely linked to apoptosis and tumor progression in numerous malignancies [8,9]. The AP-1 inhibitor T-5224, is exhibited the capability to restore the sensitivity of acute myeloid leukemia (AML) cells towards cytarabine (Ara-C) [10]. Our previous study revealed that T-5224 inhibits the proliferation and promote the apoptosis of MM cells [11]. However, T-5224-induced cell death is not fully explained by this mechanism. In this study, we further explored the mechanism by which T-5224 kills MM cells.

* Corresponding author.
E-mail address: fuyunfeng@csu.edu.cn (Y. Fu).

https://doi.org/10.1016/j.heliyon.2024.e34397
Received 13 February 2024; Received in revised form 4 July 2024; Accepted 9 July 2024
Available online 10 July 2024

Ferroptosis is a type of programmed cell death characterized by iron-dependent fatal lipid peroxidation and excessive reactive oxygen species (ROS) that differs from apoptosis, necrosis, and pyroptosis [12,13]. When cells are exposed to the ferroptosis inducer erastin, they undergo a series of distinct changes including cell membrane rupture, decreased mitochondrial volume, increased membrane density, and loss of mitochondrial cristae [14]. Glutathione peroxidase 4 (GPX4) plays a critical role in regulating lipid peroxidation and the susceptibility of cells to ferroptosis [15]. SLC7A11 and GPX4 are the most critical targets linked to the process of ferroptosis [16]. Ferroptosis is linked to several pathological and physiological events, and its potential use in cancer treatment is anticipated [17–19]. Preclinical studies have shown that ferroptosis contributes significantly to the progression of MM [20,21]. This discovery has indicated the importance of understanding the molecular mechanisms involved in MM. Therefore, initiating ferroptosis may be a prospective and innovative strategy for MM treatment.

The phosphatidylinositol-3 kinase (PI3K)/AKT signaling pathway is a critical signaling cascade that regulates diverse cellular processes including cell proliferation, growth, metabolism, and motility [22]. This signaling pathway is one of the most commonly activated pathways in cancer and maintains the biological characteristics of malignant cells [23,24]. The PI3K/AKT signaling pathway is crucial for cellular proliferation during MM progression [25,26]. Previous studies have suggested that the inhibition of specific pathways can improve the effectiveness of cancer therapy through ferroptosis induction [27]. The dual PI3K/HDAC inhibitor BEBT-908 has been demonstrated the ability to promote immunogenic ferroptosis in cancer cells, the feedback loops and crosstalk between the PI3K/AKT pathway and ferroptosis are bidirectional and complex [28]. Therefore, we hypothesize that T-5224 induces MM cell death via the PI3K/AKT signaling pathway.

Although it has been well-documented that T-5224 induces apoptosis in MM cells [11]. Due to the high mortality rate of MM cells, there are no reports regarding ferroptosis induced by T-5224 in MM cells. Therefore, we aimed to investigate the potential induction of ferroptosis by T-5224 and its related mechanisms, and to provide clinical information for treating MM. In this study, we demonstrated that T-5224 induces ferroptosis and interacts with the PI3K/AKT signaling pathway in MM cells.

2. Materials and methods

2.1. Antibodies and reagents

Antibodies specific for GPX4, SLC7A11, phospho-AKT (Ser473), AKT, Bax and Bcl2 were acquired from Abmart Pharmaceutical Technology Co., Ltd. (Shanghai, China). An anti-β-actin antibody was acquired from Proteintech.Anti-total-PI3K and anti-phospho-PI3KCA (Tyr317) antibodies were acquired from Bioss Co., Ltd. (Beijing, China). The secondary antibodies against mouse or rabbit epitopes were acquired from ApexBio (USA). Bortezomib was purchased from Selleck Chemicals (TX, USA); and ferrostatin-1 (Fer-1) and 740 Y–P (20 μM) were obtained from MedChemExpress (MCE, USA). T-5224 was purchased from ApexBio (USA).

2.2. Human myeloma cell lines and cell culture

ARP1 cells were a gift from the Cancer Research Institute of Xiangya Medical College, Central South University. ARP1 cells were authenticated using short tandem repeat (STR) analysis in 2021 and 2024. RPMI8226 cells were obtained from ATCC (Manassas, USA). RPMI8226 cells were authenticated using short tandem repeat (STR) analysis in 2022. RPMI8226-Luc cells were acquired from Shanghai Meixuan Biotechnology Co., Ltd. (Shanghai, China), which were authenticated using short tandem repeat (STR) analysis in 2021.All human cell lines are not contaminated with mycoplasma. The cell lines were cultivated in RPMI-1640 medium supplemented with 10 % FBS and 1 % penicillin/streptomycin at 37 °C with 95 % humidity and 5 % CO_2. Normal donor samples were collected after providing informed consent. The study was performed in accordance with the Helsinki Declaration, the protocol was approved by the Ethical Review Committee at the Third Xiangya Hospital, Central South University (Changsha, China), and the ethical approval number is 2018-S090.

2.3. In vitro proliferation assay

A total of 5×10^4 cells were seeded in 96-well plates. After treatment with T-5224 for 24 or 48 h. At the specified time points, 20 μl of CCK8 solution was added to each well, and the plates were further incubated at 37 °C for 2 h. The absorbance at 450 nm was measured using a multiscan spectrophotometer. The experiment was repeated three times.

2.4. Reactive oxygen species (ROS) assay

MM cells (5×10^5) were cultured in 6-well plates, treated with T-5224 for 48 h, incubated with DCFH-DA (10 μM) at 37 °C for 30 min, and then softly rinsed with warm PBS. The levels of ROS were determined by flow cytometry.

2.5. Measurement of GSH and malondialdehyde (MDA) levels

MM cells were lysed using RIPA lysis buffer (Beyotime, China) and the level of reduced glutathione was assessed using a reduced GSH detection kit (Beyotime, China). MDA levels were analyzed using a Lipid Peroxidation MDA Assay Kit (Beyotime, China) according to the manufacturer's instructions.

2.6. Western blot analysis

After being harvested, the cells were washed with PBS,lysed in RIPA buffer supplemented with 1 μM phenylmethanesulfonyl fluoride (PMSF), and centrifuged for 15 min (4 °C,12000 rpm). The protein concentrations in the supernatants were determined using a BCA protein assay kit. Subsequently, the proteins were separated via 10 % SDS–PAGE and transferred to polyvinylidene difluoride (PVDF) membranes(Millipore Corporation, Milford, Massachusetts, USA),which were further blocked with 5 % nonfat milk and washed with TBST. Afterward, the membranes were incubated overnight with primary antibodies at 4 °C, incubated for 1 h with secondary antibodies at room temperature and imaged with an imaging system (Bio-Rad, Hercules, CA, USA).

2.7. RNA-sequencing (RNA-seq) analysis

Total RNA was extracted from ARP1 cells treated with T-5224 or DMSO after two days. The cells were harvested, and total RNA was isolated using TRIzol reagent (Invitrogen, Carlsbad, CA, USA) and purified. Quality control, library construction, RNA sequencing, and bioinformatics analyses were performed by GENEWIZ (Suzhou, China). RNA-Seq was performed via the Illumina NovaSeq 6000 platform. DESeq was applied to identify differentially expressed genes (DEGs) based on a $|\log2 \text{ fold change (FC)}| > 0.5$ and adjusted $P < 0.05$.

2.8. DEGs screening

The Limma R package was utilized to identify DEGs. Which has been significantly expanded for analyzing RNA-seq data. The identification of eligible DEGs was based on the following criteria: $|\log2(FC)| > 0.5$ and adjusted $P < 0.05$ [29]. All the data were visualized by volcano plots and heatmaps using the ggplot2 and Pheatmap packages in R, respectively.

2.9. Functional enrichment analysis

For the enrichment analysis, six samples were divided into T-5224 and DMSO groups. Differential gene expression among these cohorts was determined using the limma package. The following filter criteria were applied for functional enrichment analysis: adjusted $P < 0.05$ and $|\log2FC| > 0.5$. The Kyoto Encyclopedia of Genes and Genomes (KEGG) database was utilized to identify DEGs related to specific pathways and was implemented using the ClusteProfiler package in R.

2.10. Gene set enrichment analysis (GSEA)

GSEA was performed using the R package clusterProfiler [30] to determine the functional and pathway differences between the T-5224 and DMSO groups. The enrichment analysis was performed with GSEA version 4.1.0, which involved the utilization of the hallmark gene set (h.all.v7.2.symbols.gmt). The analysis was carried out via the GSEA website(https://www.gsea-msigdb.org/gsea/index.jsp). Default settings were applied for all the other options.

2.11. Transmission electron microscopy (TEM)

The MM cells were harvested and centrifuged for 5 min (4 °C, 1000 rpm), and then fixed in 2.5 % glutaraldehyde for 2 h at 4 °C. To observe the changes in ultrastructural morphology, particularly mitochondrial ultrastructure. TEM imaging was performed by Servicebio (Wuhan, China).

2.12. Immunohistochemistry (IHC) and immunofluorescence (IF)

The tumor tissue was obtained from tumor-bearing nonobese diabetic-severe combined immunodeficient (NOD-SCID) mice, embedded in paraffin, and subsequently sectioned. Immunohistochemical staining was conducted to analyze Ki67, GPX4, SLC7A11, Bax and Bcl2 expression. Immunofluorescence was conducted to analyze the expression of TUNEL and Ki67 in the tumor tissue.

2.13. MM xenograft model

Six-week-old female NOD/SCID mice were acquired from Hunan SJA Laboratory Animal Co., Ltd. (Changsha, China). Mice were subcutaneously injected with RPMI 8226-Luc cells (5×10^5 cells/100 μl) into the left or right flanks to establish an MM xenograft model. After 10 days, when a lump had formed, the mice were randomly assigned to four different groups, with 3 mice per group, including control, T-5224, BTZ and the combination of T-5224 and BTZ groups. Some mice received intraperitoneal injections of BTZ (1 mg/kg, every 3 days) or T-5224 (20 mg/kg, every day) or the combination of T-5224 and BTZ (20 mg/kg T-5224, every day and 1 mg/kg BTZ, every 3 days) for two weeks and injections of PBS were used as a control. T-5224 was dissolved in DMSO/10 % PEG300/ddH_2O.Tumor sizes and body weights were measured every three days, and tumor volumes were calculated using the standard formula: $1/2(\text{length} \times \text{width}^2)$. Bioluminescence imaging (IVIS® Spectrum, PerkinElmer, MA, USA) was used to evaluate tumor volume. The mice were sacrificed at the completion of treatment. The Institutional Animal Care and Use Committee of Central South University sanctioned all animal experiments in this research. The approval number is CSU-2023-0147.

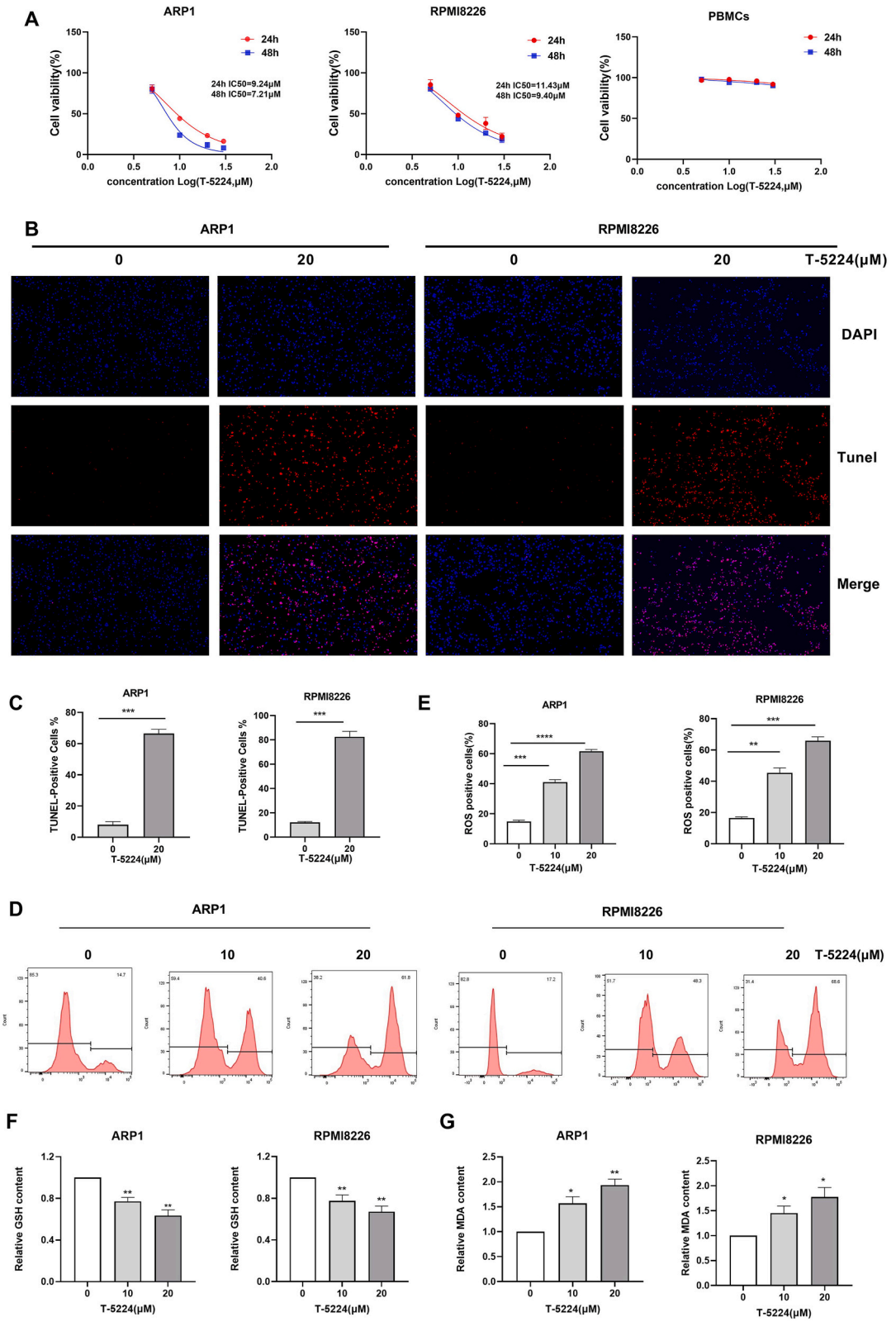

(caption on next page)

Fig. 1. T-5224 inhibited MM cell proliferation. (A) MM cell lines and PBMCs derived from healthy donors were exposed to various concentrations of T-5224 (5, 10, or 20 μmol/L) for 24 h or 48 h, after which cell viability was evaluated by the CCK-8 assay. **(B)** MM cells stained with TUNEL (red) and DAPI (blue), are depicted in the provided images. (scale bar, 50 μm) **(C)** Quantitative analysis was conducted. **(D–E)** MM cells were exposed to various concentrations of T-5224 for 48 h, and the production of ROS was measured by flow cytometry. *P < 0.05, **P < 0.01, ***P < 0.001, ****P < 0.0001 vs. Control. **(F–G)** The relative levels of reduced GSH and increased MDA in MM cells. *P < 0.05, **P < 0.01, ***P < 0.001, ****P < 0.0001 vs. Control. The results are presented as the mean ± standard deviation (SD). (For interpretation of the references to colour in this figure legend, the reader is referred to the Web version of this article.)

2.14. Hematoxylin–eosin (HE) staining

The primary organs of the mice were harvested, preserved in 4 % paraformaldehyde, then embedded in paraffin and sectioned. Five-micrometer-thick sections were subjected to histological examination by H&E staining.

2.15. Statistical analyses

The data were analyzed using R 3.6.1 and GraphPad Prism 7.0 software (GraphPad Software, La Jolla, CA, USA). All results are presented as the mean ± standard deviation (SD), and comparisons among two groups were evaluated by Student's t-test. Differences among three or more groups were evaluated by one-way ANOVA. $P < 0.05$ was considered to indicate statistical significance.

3. Results

3.1. T-5224 exhibits anti-MM properties in vitro

T-5224 exhibits antitumor effects on various malignant tumor types [8–11]. Our previous study indicated that T-5224 inhibits proliferation and promotes apoptosis induced cell death in MM cells [11]. We aimed to further investigate more possibilities regarding whether T-5224 can induce alternative forms of cell death. MM cells and peripheral blood mononuclear cells (PBMCs) were exposed to T-5224 or DMSO for 48 h. The effect of AP-1 inhibitors on cell viability was evaluated (Fig. 1A). Our results indicated that T-5224 exhibited significant antimyeloma effects in a dose-dependent manner, but had nearly no effect on PBMCs isolated from healthy donors. Furthermore, TUNEL staining revealed that, the T-5224 group had a greater percentage of TUNEL-positive cells than did the control group (Fig. 1B and C). Ferroptosis leads to various cellular alterations, including the accumulation of ROS, Subsequently, we identified changes in the generation of ROS produced during ferroptosis. The results revealed that T-5224 increased ROS levels in MM cells (Fig. 1D and E). Subsequently, we determined that compared with the control, T-5224 led to a reduction in the level of GSH and increased the level of one of the final products of excess lipid oxidation MDA (Fig. 1F and G).Thus,T-5224 inhibits proliferation and induces ferroptosis in MM cells.

3.2. T-5224 exhibits anti-MM properties in vivo

Based on our in vitro experimental results, we aimed to investigate whether T-5224 can suppress the growth and proliferation of an RPMI8226-luc cell-derived xenograft mouse model. RPMI8226-luc cells were subcutaneously injected into either the left or right flank of mice to establish an MM xenograft model, and the tumor-bearing mice were subsequently treated with 20 mg/kg T-5224(Fig. 2A). As expected, compared with those in the control group, the tumor sizes in the T-5224-treated group were markedly reduced (Fig. 2B). In addition, we observed a notable decrease in tumor volume relative to that in the control group (Fig. 2C). Furthermore, the tumor-bearing mice treated with T-5224 did not exhibit significant weight loss during treatment, which indicates no notable toxicity. (Fig. 2D). The immunohistochemistry results demonstrated that treatment with T-5224 had a significant impact on ferroptosis and apoptosis biomarkers (GPX4, SLC7A11, Bcl2, and Bax) in tumor tissues. As expected, T-5224 treatment decreased GPX4, SLC7A11 and Bcl2 expression and increased Bax expression in tumor tissues (Fig. 2E). Additionally, compared to those in the control group, H&E staining revealed that T-5224 (20 mg/kg) did not cause discernible damage to the heart, liver, spleen, or kidneys of the tumor-bearing mice (Fig. 2F). This finding indicated that T-5224 suppresses tumor growth and initiates the ferroptosis signaling pathway in vivo. This evidence indicates that T-5224 inhibits the growth of MM cells in vivo, without causing any adverse reactions.

3.3. RNA-seq revealed that T-5224 regulates the expression of related genes and pathways

To systematically investigate the potential molecular mechanisms by which T-5224 modulates gene expression, we next conducted RNA-Seq to analyze the transcriptomes of T-5224-treated cells and the changes in gene expression. We identified a total of 1328 DEGs between T-5224-treated and DMSO-treated cells. With the DMSO group as the reference, 619 (46.6 %) genes and 709 (53.4 %) genes were found to be upregulated and downregulated, respectively, in the T-5224 group. A heatmap and volcano plot were generated to visualize the overlapping DEGs between the T-5224 and DMSO groups (Fig. 3A and B). The expression heatmap of the top 100 DEGs of these 1328 genes (Fig. 3C). We then performed KEGG analysis of the DEGs that might participate in cancer related pathways. The analysis revealed potential associations with pathways in cancer and the PI3K/AKT signaling pathway, and the critical role of the PI3K/AKT signaling pathway is well recognized in MM cells [25,26].The results of the analysis are presented in Table 1 and Fig. 3D and E. We next further verified these findings.

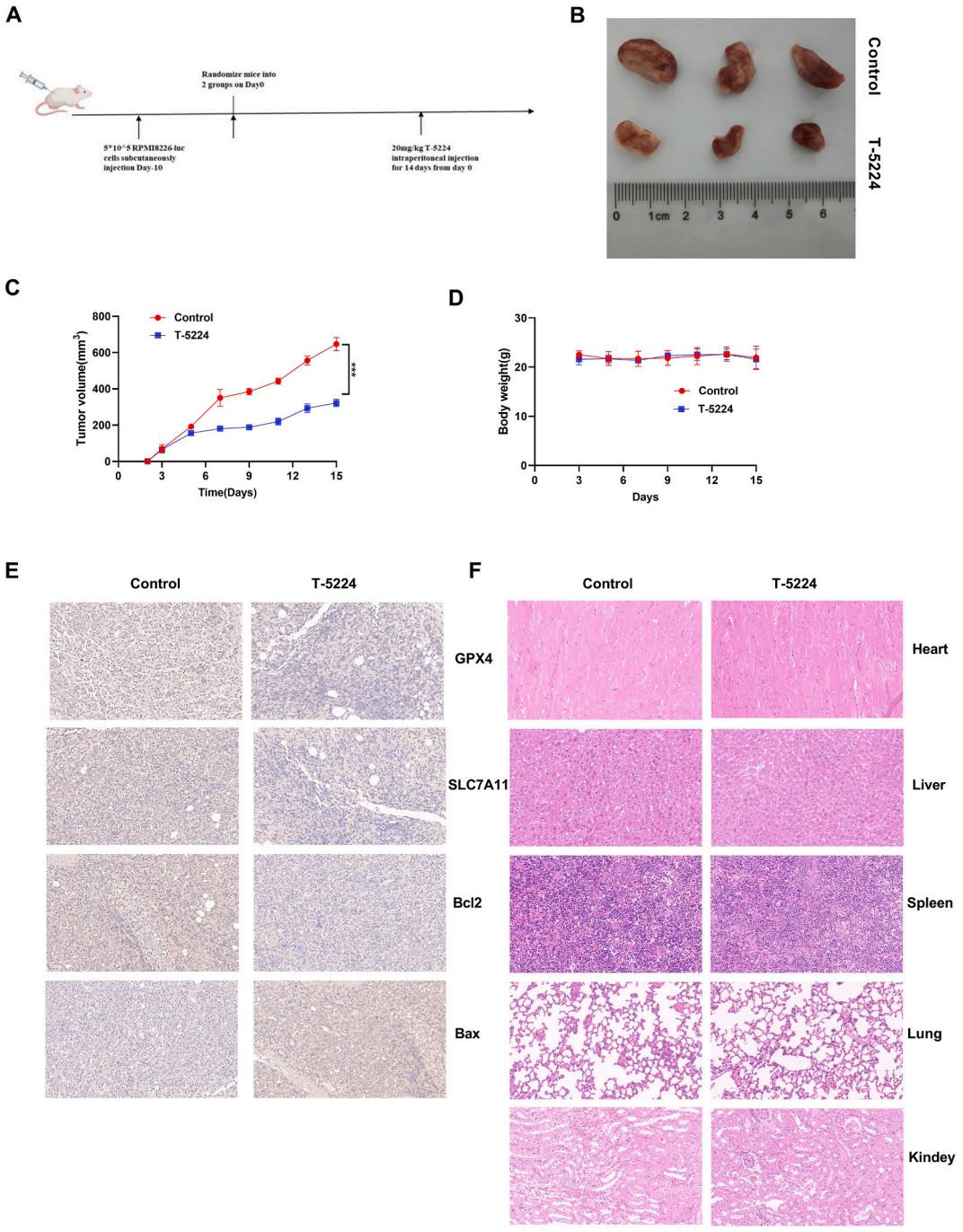

Fig. 2. T-5224 exerts antitumor effects in an MM xenograft model. (A) The diagram illustrates the process of treating MM with T-5224 in vivo. **(B)** The representative images of RPMI8226-luc xenograft tumors were captured after T-5224 treatment (n = 3). **(C)** The tumor volume was measured in each group. *P < 0.05, **P < 0.01, ***P < 0.001 vs. Control. **(D)** The body weights of the xenograft model mice were measured after T-5224(20 mg/kg) treatment. **(E)**Representative images of GPX4, SLC7A11, Bcl2 and Bax immunohistochemical staining were obtained from tumor tissues in each group. (scale bars: 50 μm) **(F)** HE staining was conducted to assess histopathological alterations in primary organs from MM xenograft mice. The results are presented as the mean ± standard deviation (SD).

3.4. T-5224 induces ferroptosis in MM cells

Ferroptosis has become a hot topic, particularly in the context of cancer and MM [19–21]. In a previous study, T-5224 was shown to inhibit proliferation and induced apoptosis, causing cell death in MM cells [11]. However, the high mortality cannot be fully explained,

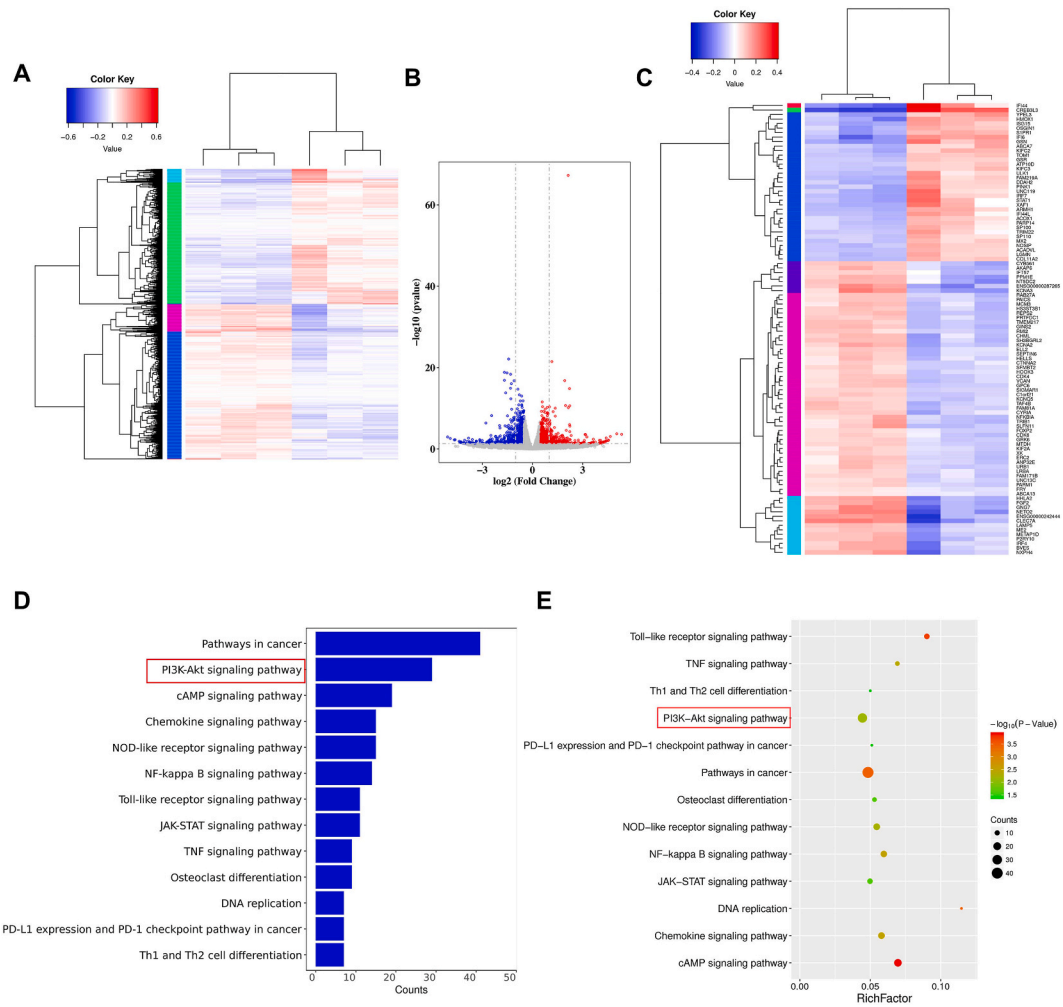

Fig. 3. T-5224 regulates the expression of different genes and pathways. (A) The heatmap illustrates the DEGs according to the |log2FC| value. **(B)** The volcano plot illustrates the DEGs between T-5224 group and DMSO group. Red plots represent upregulated expression, blue plots represent downregulated expression, and gray plot indicate no difference in expression. **(C)** Heatmap displaying the distribution of the top hundred DEGs. **(D)** Bar chart of KEGG enrichment. The vertical axis shows the details of the enriched pathways and the horizontal axis shows the count of DEGs in the pathway relative to the total count of DEGs. **(E)** KEGG enrichment analysis of T-5224 and DMSO. (For interpretation of the references to colour in this figure legend, the reader is referred to the Web version of this article.)

Table 1
Kyoto Encyclopedia of Genes and Genomes enrichment analysis results ($P < 0.05$).

ID	Pathway	Counts	P value
ko05200	Pathways in cancer	41	3.56E-04
ko04151	PI3K-Akt signaling pathway	29	7.09E-03
ko04024	cAMP signaling pathway	19	1.15E-04
ko04062	Chemokine signaling pathway	15	3.19E-03
ko04621	NOD-like receptor signaling pathway	15	5.67E-03
ko04064	NF-kappa B signaling pathway	14	3.12E-03
ko04620	Toll-like receptor signaling pathway	11	1.90E-04
ko04630	JAK-STAT signaling pathway	11	2.49E-02
ko04668	TNF signaling pathway	9	4.07E-03
ko04380	Osteoclast differentiation	9	2.40E-02
ko03030	DNA replication	7	3.21E-04
ko05235	PD-L1 expression and PD-1 checkpoint pathway in cancer	7	4.25E-02
ko04658	Th1 and Th2 cell differentiation	7	4.72E-02

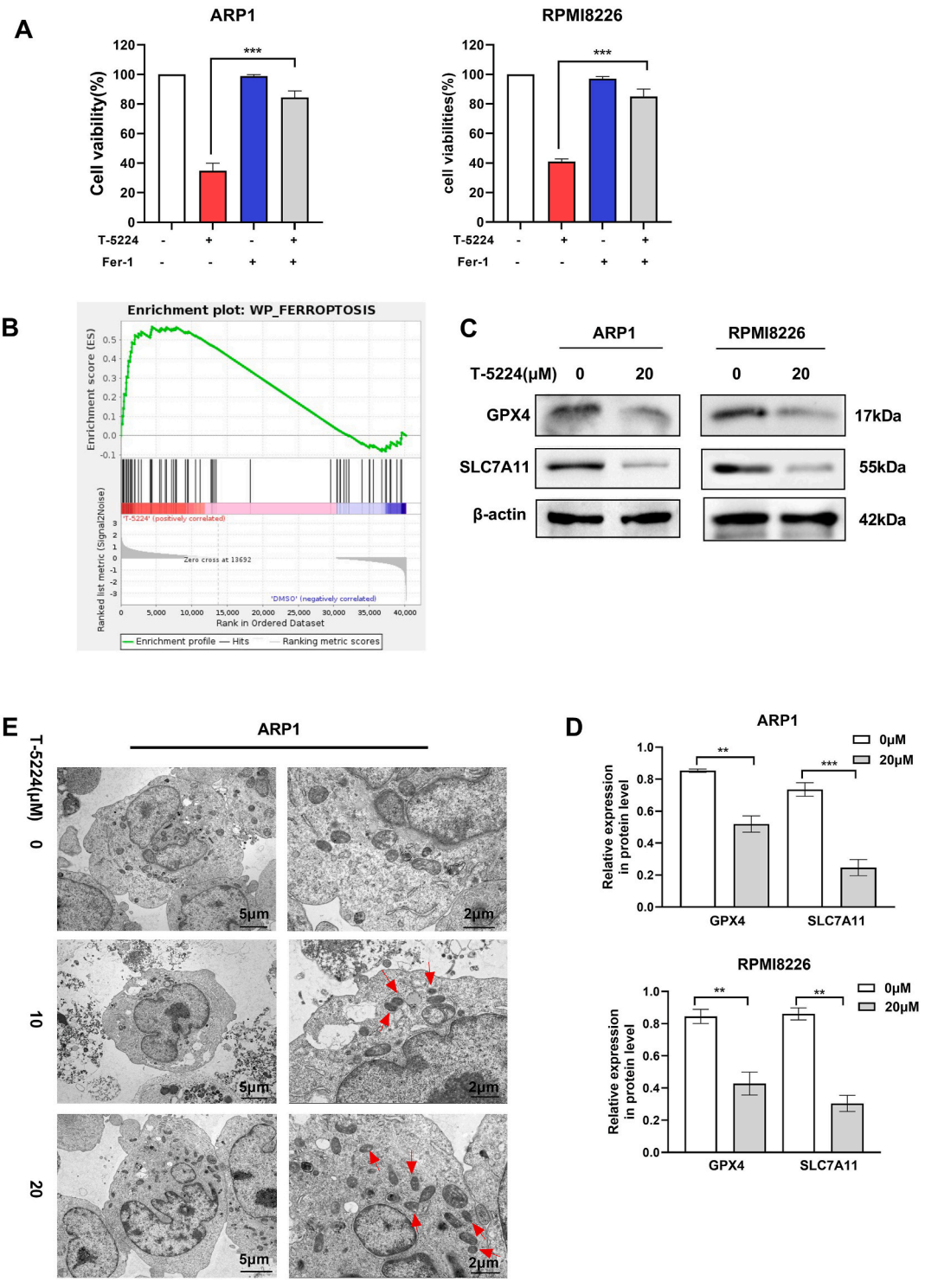

(caption on next page)

Fig. 4. T-5224 induces ferroptosis in MM cells. (A) MM cells were exposed to T-5224 (20 μM) in the presence or absence of the ferroptosis inhibitor Fer-1 (5 μM) for 48 h, after which cell viability was evaluated by the CCK-8 assay. *P < 0.05, **P < 0.01, ***P < 0.001 for T-5224 vs. T-5224 in combination with Fer-1**(B)** GSEA was conducted on the T-5224 group and DMSO group. **(C)** The protein levels of GPX4 and SLC7A11 in MM cells were evaluated by western blotting. β-actin served as the protein loading control. **(D)** The histogram displays the relative gray values. *P < 0.05, **P < 0.01, ***P < 0.001 vs. Control **(E)**Transmission electron microscopy (TEM) was utilized to observe the occurrence of ferroptosis before and after T-5224 treatment in MM cells. Red arrowheads: mitochondrial crista destruction, which occurs during the iron death stage. The results are presented as the mean ± standard deviation (SD). (For interpretation of the references to colour in this figure legend, the reader is referred to the Web version of this article.)

and our objective was to further investigate more possibilities regarding whether T-5224 can induce other forms of cell death. We treated MM cells with cell death inhibitors and then treated them with T-5224. Fer-1, a ferroptosis specific inhibitor, reversed T-5224-induced cell death in MM cells (Fig. 4A). To further clarify the signaling pathways associated with T-5224 in MM cells, we analyzed the DEGs between the T-5224 and DMSO groups using GSEA. Ferroptosis was enriched, indicating that the ferroptosis pathway may be involved (Fig. 4B). Previous studies have demonstrated that GPX4 and SLC7A11 are inactivated and depleted, and can inhibit cysteine metabolism, which results in increased lipid peroxidation and the occurrence of ferroptosis [20,21,31,32].These findings indicate that decreased GPX4 and SLC7A11 expression is indicative of ferroptosis. Subsequently, we investigated the influence of T-5224 on ferroptosis-related proteins (SLC7A11 and GPX4) by western blotting, and the results indicated that SLC7A11 and GPX4 were effectively inhibited by T-5224 at the protein level in MM cells (Fig. 4C and D). Transmission electron microscopy (TEM) was used to examine the morphological characteristics of cells undergoing ferroptosis. The results revealed that T-5224 triggered shrunken mitochondrial volume and increased the membrane density in MM cells (Fig. 4E), indicating the occurrence of ferroptosis.

3.5. T-5224 triggers ferroptosis in MM cells by inhibiting the PI3K/AKT signaling pathway

The phosphatidylinositol 3-kinase-protein kinase B (PI3K/AKT) signaling pathway is known to participate in the process of cell death [26].Excessive activation of the PI3K/AKT signaling pathway facilitates malignant transformation of cells by regulating numerous cellular processes, including tumor cell proliferation, apoptosis, immune evasion and drug resistance [22,33]. To elucidate the mechanisms underlying the antimyeloma effects of T-5224, we performed RNA-Seq and KEGG analyses. The results (Fig. 3E)

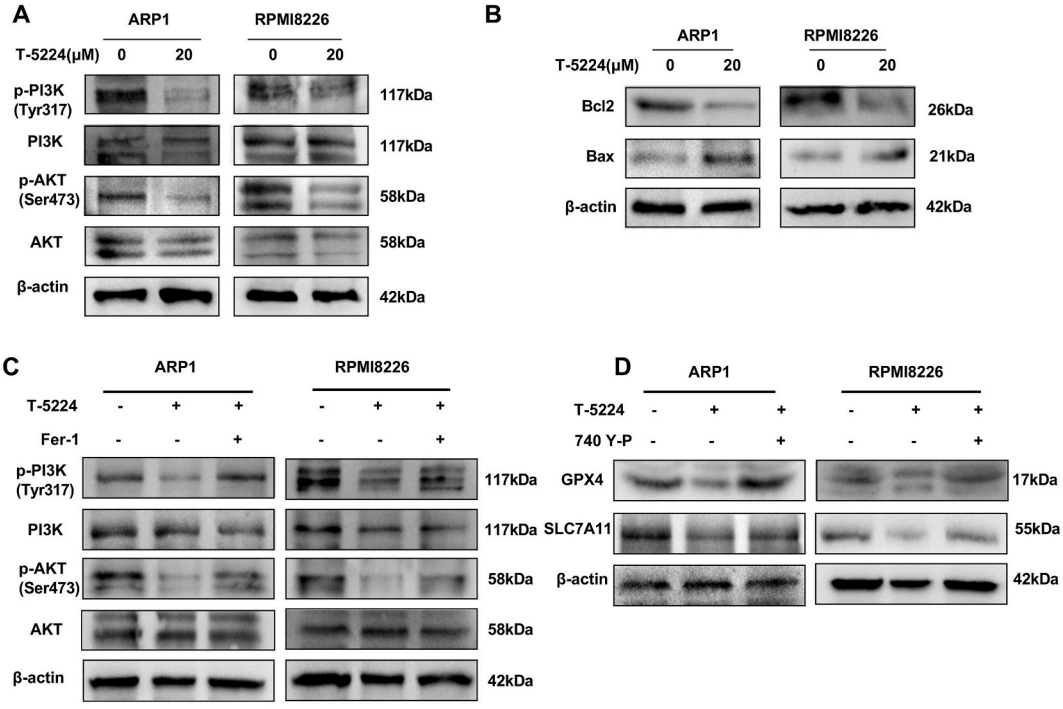

Fig. 5. The PI3K/AKT signaling pathway is involved in AP-1 inhibitor-induced ferroptosis. (A) MM cells were exposed to T-5224 (20 μM) for 48 h. The protein levels of *p*-AKT(Ser473), total AKT, p-PI3K (Tyr317), and total PI3K were assessed by western blotting. **(B)** MM cells were exposed to T-5224 (20 μM) for 48 h. The protein levels of Bcl2 and Bax in MM cells were assessed by western blotting. **(C)** MM cells were exposed to T-5224 in the presence or absence of Fer-1 (5 μM) for 48 h, after which the protein levels of *p*-AKT(Ser473), AKT, p-PI3K (Tyr317), and PI3K were assessed by western blotting. **(D)** MM cells were exposed to T-5224(20 μM) in the presence or absence of 740 Y–P (20 μM) for 48 h. The protein levels of GPX4 and SLC7A11 in MM cells were assessed by western blotting. β-actin served as the protein loading control. The results are presented as the mean ± standard deviation (SD).

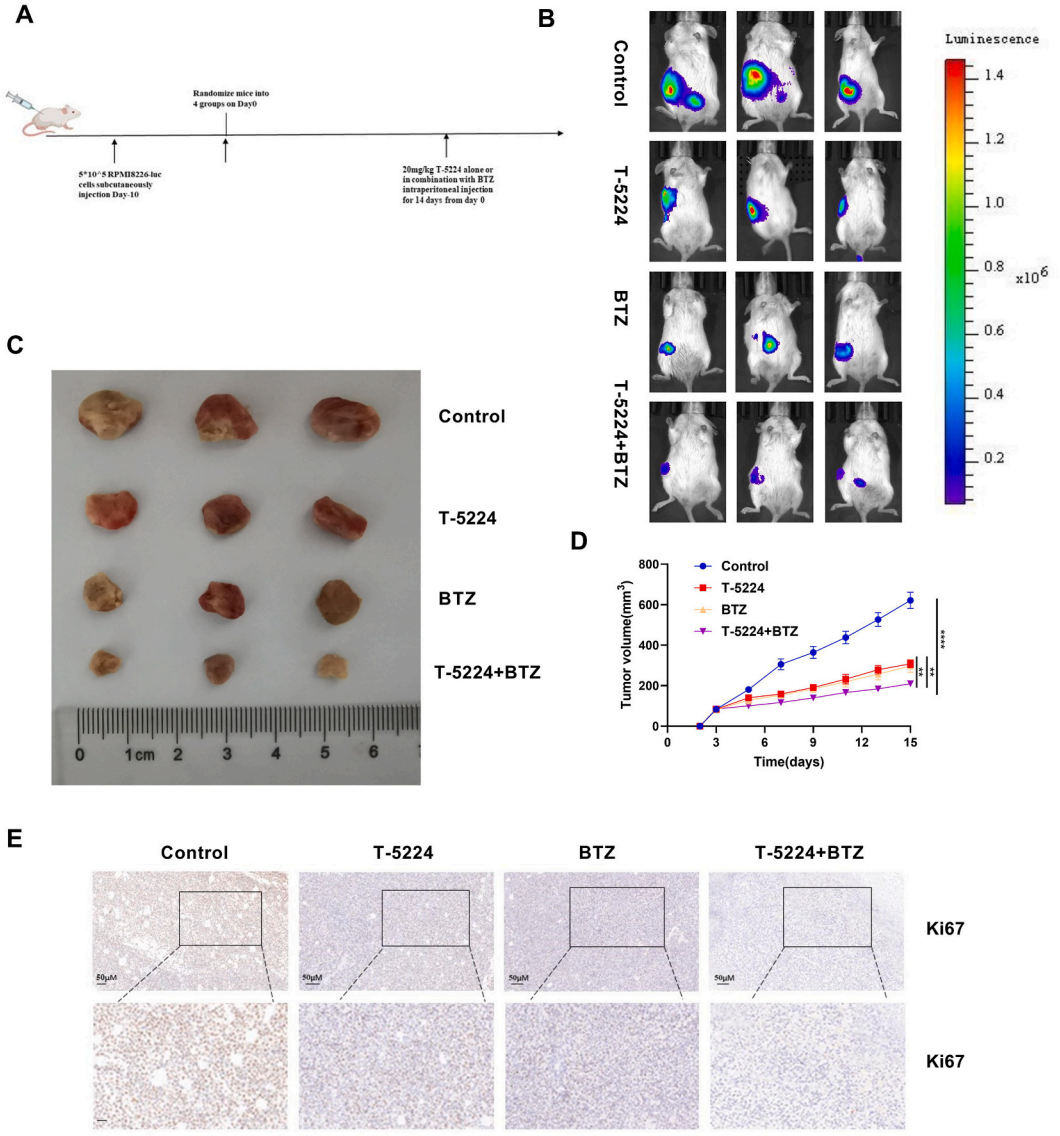

Fig. 6. The combination of T-5224 and BTZ exerts more potent antimyeloma activity in vivo. (A) The diagram illustrates the process of MM treatment with T-5224 alone or in combination with BTZ in vivo. **(B)** The quantification of tumor cells in mice was conducted using bioluminescence analysis. Bioluminescence images of mice treated with PBS, T-5224 (20 mg/kg), BTZ (1 mg/kg) or the combination of T-5224 and BTZ at the indicated time points.**(C)** Representative images of RPMI8226-luc xenograft tumors were captured after different treatments **(D)** The tumor volume was measured for each group. *P < 0.05, **P < 0.01, ***P < 0.001, ****P < 0.0001 The combination of T-5224 and BTZ vs. Control, T-5224/BTZ vs. The combination of T-5224 and BTZ. **(E)** The representative images of Ki67 immunohistochemical staining were obtained from tumor tissues in each group. (scale bars: 50 μm). **(F–G)** The representative images of mouse tumor tissues stained with TUNEL (red) and DAPI (blue) (scale bar, 50 μm). *P < 0.05, **P < 0.01, ***P < 0.001, ****P < 0.0001 The combination of T-5224 and BTZ vs. Control, T-5224/BTZ vs. The combination of T-5224 and BTZ. **(H–I)** The representative images of Ki67 immunofluorescence staining were obtained from tumor tissues in each group. (scale bars: 50 μm). *P < 0.05, **P < 0.01, ***P < 0.001, ****P < 0.0001 The combination of T-5224 and BTZ vs. Control, T-5224/BTZ vs. The combination of T-5224 and BTZ. The results are presented as the mean ± standard deviation (SD). (For interpretation of the references to colour in this figure legend, the reader is referred to the Web version of this article).

revealed that the PI3K/AKT signaling pathway may be significantly involved in the anticancer bioactivity of T-5224 in MM cells. Western blot analysis confirmed that T-5224 reduced the phosphorylation of PI3K at the Tyr317 site, and further dephosphorylated AKT at the Ser473 site, while total PI3K and total AKT expression were unchanged, suggesting that the PI3K/AKT signaling pathway may be involved in T-5224-induced cell death in MM cells (Fig. 5A). Additionally, T-5224 downregulated Bcl2 expression and upregulated Bax expression, thereby promoting the activation of intrinsic apoptotic pathways in MM cells (Fig. 5B). Inhibition of the PI3K/AKT signaling pathway can induce ferroptosis in cancer cells [27,28]. Our results indicated that T-5224 induced ferroptosis in

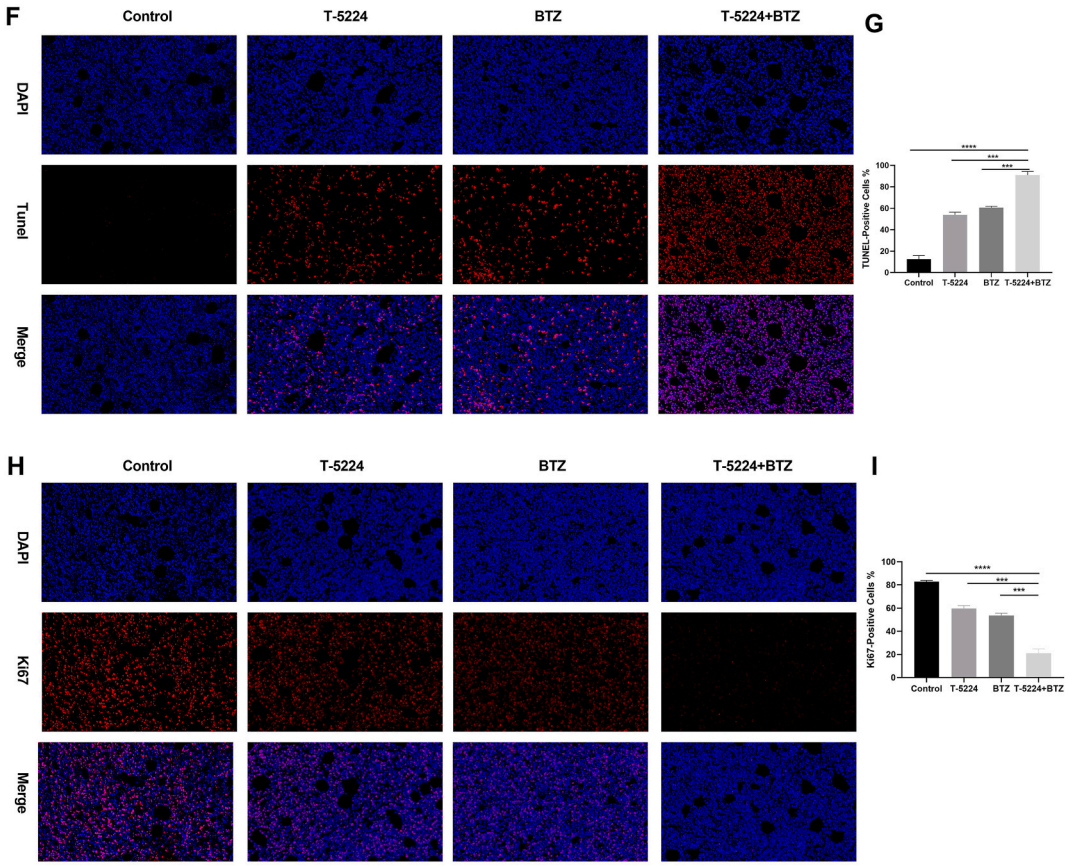

Fig. 6. (*continued*).

MM cells. Hence, we postulated that T-5224 might induce ferroptosis by inhibiting the PI3K/AKT signaling pathway. To verify this hypothesis, we selected 740-Y-P, a PI3K/AKT activator, and Fer-1, a ferroptosis inhibitor, for subsequent experimental investigations. MM cells were subjected to treatment with Fer-1 in the presence or absence of T-5224, and the findings demonstrated that Fer-1 reversed the inhibition of the PI3K/AKT pathway triggered by T-5224 in MM cells (Fig. 5C). We found that the PI3K/AKT pathway activator 740 Y–P reversed the T-5224-induced decrease in GPX4 and SLC7A11 expression (Fig. 5D); therefore, we inferred that the activation of the PI3K/AKT signaling pathway by 740 Y–P inhibited ferroptosis induced by T-5224.In conclusion, these findings indicated that T-5224 triggered ferroptosis via the PI3K/AKT signaling pathway in MM cells.

3.6. AP-1 inhibitors combined with proteasome inhibitors significantly inhibit MM tumor growth in vivo

BTZ has become a widely used first-line therapeutic agent for MM treatment. Our previous findings showed that the combination of T-5224 and BTZ has synergistic cytotoxic effects on MM cells by suppressing the IRF4/MYC axis pathway in vitro [11]. Based on the results of the in vitro experiments, a xenograft model was constructed by subcutaneously injecting RPMI8226-luc cells into SOD/SCID mice, which were then treated with T-5224 (20 mg/kg) monotherapy or in combination with BTZ (Fig. 6A). The experiment involved the random division of mice into four different groups, including control, T-5224, BTZ, and the combination of T-5224 and BTZ. We further studies were conducted in MM xenograft mice.

The tumor burden evaluated by luciferase activity, was significantly lower in the mice treated with the combination of T-5224 and BTZ than in the mice in the control, T-5224 and BTZ groups (Fig. 6B). The combined treatment led to a significant reduction in tumor burden, as indicated by a decrease in tumor volume. (Fig. 6C and D). This finding indicates the significant inhibitory effect of the combination treatment on tumor growth.

Furthermore, the immunohistochemistry results showed that the combination treatment resulted in significantly fewer Ki67 (a proliferation marker) positive cells (Fig. 6E). The immunofluorescence results (Fig. 6G) were similar to the immunohistochemistry results. Furthermore, the impact of T-5224 on apoptosis was investigated by using TUNEL staining. The combination group exhibited a greater percentage of TUNEL-positive cells than did the control group, T-5224 and BTZ groups (Fig. 6F). Overall, these findings demonstrated that the combination of T-5224 and BTZ is highly effective in vivo.

3.7. Evaluation of the safety of T-5224 combined with bortezomib in vivo

To assess the toxicity of various drugs in vivo, MM xenograft mice were subjected to various treatments including PBS, T-5224, BTZ, or the combination of T-5224 and BTZ. This drug combination had no notable toxicity at the applied doses, and the mice did not show significant reductions during treatment (Fig. 7A). On the 14th post-injection day, all the mice were euthanized, and their blood and primary organs were harvested for further examination. Histological evaluation via H&E staining revealed that compared with the control treatment, BTZ monotherapy, T-5224 monotherapy and combined T-5224 and BTZ treatment showed no discernible pathological alterations in the heart, liver, spleen, or kidneys of the mice (Fig. 7B). These findings indicate that the combination of T-5224 and BTZ has low toxicity and minimal adverse reactions in vivo. In summary, these findings indicate that the combined therapy was well tolerated.

4. Discussion

Despite the approval of novel drugs for MM treatment, MM patients are still considered incurable [34]. Addressing these challenges is crucial for improving clinical outcomes. T-5224, a selective AP-1 inhibitor, is promising for treating arthritis [6]. Research has demonstrated its promising therapeutic potential for various types of cancer [8,9]. We confirmed the antimyeloma effect of T-5224 in vitro, confirming its initial therapeutic potential [11]. However, the high mortality cannot be fully explained, and this study aimed to investigate whether T-5224 could induce other forms of cell death. Therefore, we conducted a comprehensive exploration both in vitro and in vivo.

Ferroptosis is a novel form of cell death associated with multiple apoptotic mechanisms, and is characterized by lipid peroxidation and iron accumulation. The process of ferroptosis involves the regulation of numerous genes and signaling pathways, leading to a cascade of intricate biochemical reactions [35,36]. Recent research has demonstrated the efficacy of ferroptosis inducers in killing tumor cells [37]. Compared with normal cells, cancer cells exhibit greater iron requirements, and this dependence on iron increases susceptibility to ferroptosis [38]. In this study, we found that T-5224 is correlated with ferroptosis in MM cells, highlighting the crucial importance of ferroptosis in MM progression. Ferroptosis is a nonapoptotic form of cell death, that is induced by the aggregation of ROS [39,40].In terms of morphology, ferroptosis leads to the mitochondria in cells undergo shrinkage, increased density of the mitochondrial membrane, and destruction of mitochondrial ridges [20]. GPX4 and SLC7A11 have been identified as crucial regulators of ferroptosis, when GPX4 and SLC7A11 expression is low, resulting in the accumulation of ROS and subsequent ferroptosis [31,32,41]. The levels of GPX4 and SLC7A11 are reduced, resulting in an imbalance in ROS production and elimination [20]. We found that T-5224 increased the levels of ROS and MDA, and reduced the level of GSH in MM cells; moreover, T-5224 effectively inhibited GPX4 and SLC7A11 expression in MM cells. Fer-1 treatment prevented T-5224 induced MM cell death, indicating the occurrence of ferroptosis. These results suggest that T-5224 exerts its potential anticancer effects by inducing ferroptosis in MM cells. All of these findings provide evidence for its clinical application in the future.

The PI3K/AKT axis is crucial for cancer cell survival in various malignancies, including MM. Previous research has shown that it regulates cellular physiology, including cancer cell proliferation, metabolism, survival, and protein synthesis [42]. Activation of the PI3K/AKT signaling pathway is associated with the metastasis of bladder cancer (BLCA) cells [24]. Additionally, the involvement of

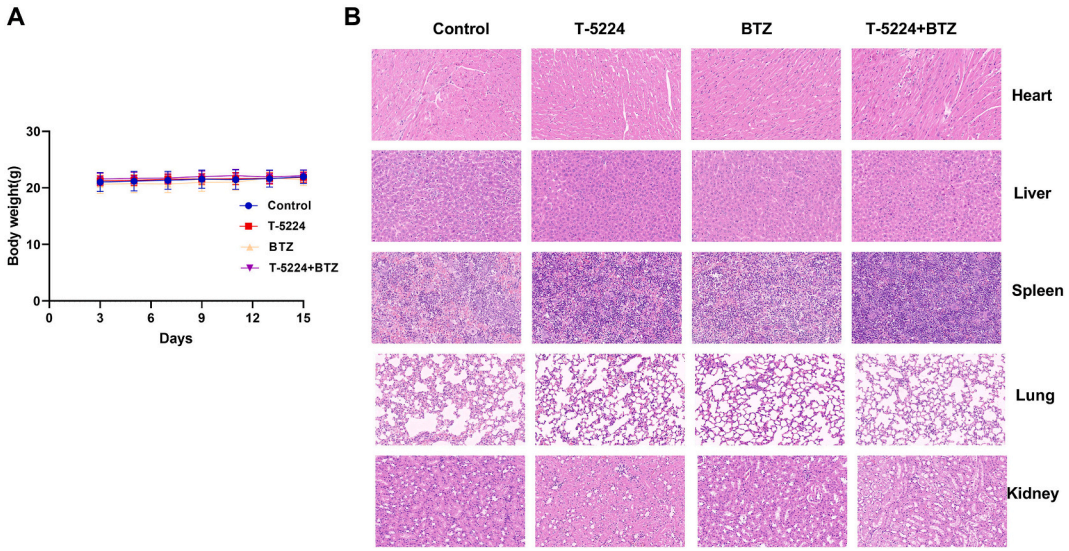

Fig. 7. The combination of T-5224 and BTZ exhibited unremarkable organ toxicity in SOD/SCID mice. (A) The body weights of the MM xenograft mice were measured after treatment with PBS, T-5224(20 mg/kg), BTZ (1 mg/kg) or the combination of T-5224 and BTZ. **(B)** HE staining was conducted to assess histopathological alterations in primary organs from the MM xenograft mice. (scale bars: 50 μm).

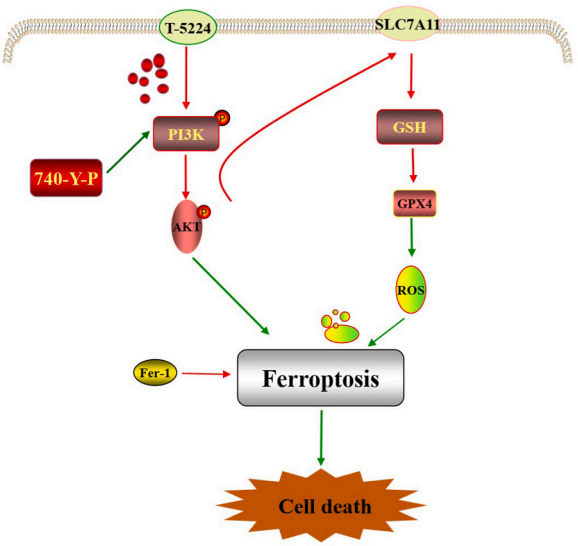

Fig. 8. Summary of T-5224 induces ferroptosis via the PI3K/AKT signaling pathway in MM cells. T-5224 inhibits the PI3K/AKT signaling pathway, leading to the inhibition of SLC7A11 and GPX4 expression. A reduction in SLC7A11 and GPX4 leads to decreased clearance of ROS, ultimately causing an increase in ROS levels and subsequent ferroptosis in MM cells. This leads to MM cell death. 740-Y-P is a PI3K/AKT activator, and Fer-1 is a ferroptosis inhibitor. The red arrow and green arrow represent inhibiting and promoting effects, respectively. (For interpretation of the references to colour in this figure legend, the reader is referred to the Web version of this article.)

the PI3K/AKT/mTOR pathway in cancer has been demonstrated through its regulation of ferroptosis [28,43]. According to Zhao et al. [26], the inhibition of PI3K induced ferroptosis in MM cells. However, the specific impact of T-5224 on ferroptosis via the PI3K/AKT signaling pathway remains unclear. Our RNA-Seq analysis revealed the downstream targets of AP-1 and the underlying molecular mechanism in MM cells following T-5224 treatment. RNA-Seq and KEGG analyses demonstrated that the DEGs between the T-5224 and DMSO groups were enriched in the PI3K/AKT signaling pathway in MM cells. Furthermore, we confirmed that T-5224 inhibited the phosphorylation of PI3K(Tyr317) and AKT(Ser473), and ultimately caused MM cell death, indicating the crucial role of the PI3K/AKT signaling pathway in the regulatory processes of T-5224 in MM cells. Mechanistically, Fer-1, a ferroptosis inhibitor, reversed T-5224-induced inactivation of the PI3K/AKT signaling pathway in MM cells, highlighting the crucial and innovative role of ferroptosis in MM treatment. Moreover, the activation of this pathway reversed the decreases in GPX4 and SLC7A11 expression induced by T-5224. Therefore, the PI3K/AKT signaling pathway at least partly mediates ferroptosis. Our study provides evidence that T-5224 deactivates the PI3K/AKT signaling pathway and ultimately induces ferroptosis (Fig. 8).

BTZ is a first-in-class proteasome inhibitor for treating MM. Clinical studies have indicated that compared with intravenous injection, subcutaneous injection of BTZ can reduce the occurrence of adverse events, while maintaining similar overall response rates [44,45].In preclinical animal studies, BTZ has been shown to induce tail vein injury and occlusion in mice, making drug administration challenging. Consequently, many studies have administered BTZ intraperitoneally by injection in animal models [45,46]. Previous studies have shown that the combination of T-5224 and BTZ is more cytotoxic than T-5224 monotherapy in vitro [11]. In this study, we demonstrated that T-5224 reduced the tumor burden in MM xenograft mice, and synergistically promoted the antimyeloma effect of BTZ in vivo, consistent with previous in vitro experiments. Moreover, compared with the control group, the combined treatment group did not exhibit obvious weight loss. HE staining did not reveal signs of visceral injury in the combined treatment group, confirming the safety of using this therapeutic approach in vivo.

5. Conclusions

In conclusion, our study showed that T-5224 suppressed the proliferation and growth of MM cells both in vivo and in vitro. Mechanistically, T-5224 inhibited the PI3K/AKT signaling pathway and ultimately induced ferroptosis, at least partially contributing to its anticancer effects. Our findings provide a preclinical foundation and insights for the potential application of T-5224 as a therapeutic agent in MM management. We aimed to provide a novel perspective for the field of MM treatment.

However, a limitation of this study is that we did not collect additional measurement parameters from the mice. Future studies are needed to thoroughly consider all relevant factors to provide more comprehensive results.

Ethics declarations

Normal donor samples were collected after providing informed consent. The study was performed in accordance with the Helsinki Declaration, the protocol was approved by the Ethical Review Committee at the Third Xiangya Hospital, Central South University

(Changsha, China), and the ethical approval number is 2018-S090. The Institutional Animal Care and Use Committee of Central South University sanctioned all animal experiments in this research. the approval number is CSU-2023-0147.

Fundings

This study was supported by the National Natural Science Foundation of China (Grant Nos. 81870166) and the Natural Science Foundation of Hunan Province (Grant Nos.2022JJ30885)

Data availability statement

Data will be made available on request.

CRediT authorship contribution statement

Sishi Tang: Writing – review & editing, Writing – original draft, Validation, Software, Resources, Methodology, Investigation, Formal analysis, Data curation. **Jing Liu:** Writing – review & editing, Supervision, Resources, Project administration, Investigation, Funding acquisition, Conceptualization. **Fangfang Li:** Validation, Software, Resources, Investigation, Data curation. **Yuhan Yan:** Validation, Project administration, Methodology, Formal analysis, Data curation, Conceptualization. **Xinyi Long:** Validation, Software, Investigation. **Yunfeng Fu:** Writing – review & editing, Visualization, Supervision, Resources, Project administration, Methodology, Investigation, Funding acquisition.

Declaration of competing interest

The authors declare that they have no known competing financial interests or personal relationships that could have appeared to influence the work reported in this paper.

Acknowledgements

Thanks for all participants involved in this study.

Appendix A. Supplementary data

Supplementary data to this article can be found online at https://doi.org/10.1016/j.heliyon.2024.e34397.

References

[1] T. Hideshima, C. Mitsiades, G. Tonon, P.G. Richardson, K.C. Anderson, Understanding multiple myeloma pathogenesis in the bone marrow to identify new therapeutic targets, Nat. Rev. Cancer 7 (8) (2007) 585–598, https://doi.org/10.1038/nrc2189.
[2] S.V. Rajkumar, M.A. Dimopoulos, A. Palumbo, et al., International Myeloma Working Group updated criteria for the diagnosis of multiple myeloma, Lancet Oncol. 15 (12) (2014) e538–e548, https://doi.org/10.1016/S1470-2045(14)70442-5.
[3] J. Silberstein, S. Tuchman, S.J. Grant, What is multiple myeloma? JAMA 327 (5) (2022) 497, https://doi.org/10.1001/jama.2021.25306.
[4] N. van de Donk, C. Pawlyn, K.L. Yong, Multiple myeloma, Lancet 397 (10272) (2021) 410–427, https://doi.org/10.1016/S0140-6736(21)00135-5.
[5] P.G. Richardson, S.J. Jacobus, E.A. Weller, et al., Triplet therapy, transplantation, and Maintenance until progression in myeloma, N. Engl. J. Med. 387 (2) (2022) 132–147, https://doi.org/10.1056/NEJMoa2204925.
[6] Y. Aikawa, K. Morimoto, T. Yamamoto, et al., Treatment of arthritis with a selective inhibitor of c-Fos/activator protein-1, Nat. Biotechnol. 26 (7) (2008) 817–823, https://doi.org/10.1038/nbt1412.
[7] H.N. Wang, K. Ji, L.N. Zhang, et al., Inhibition of c-Fos expression attenuates IgE-mediated mast cell activation and allergic inflammation by counteracting an inhibitory AP1/Egr1/IL-4 axis, J. Transl. Med. 19 (1) (2021) 261, https://doi.org/10.1186/s12967-021-02932-0.
[8] R. Liu, J. Tan, X. Shen, et al., Therapeutic targeting of FOS in mutant TERT cancers through removing TERT suppression of apoptosis via regulating survivin and TRAIL-R2, Proc. Natl. Acad. Sci. U.S.A. 118 (11) (2021), https://doi.org/10.1073/pnas.2022779118.
[9] S. Zhao, B. Li, R. Zhao, et al., Hypoxia-induced circADAMTS6 in a TDP43-dependent manner accelerates glioblastoma progression via ANXA2/NF-kappaB pathway, Oncogene 42 (2) (2023) 138–153, https://doi.org/10.1038/s41388-022-02542-0.
[10] H. Wang, H. Zhan, X. Jiang, et al., A novel miRNA restores the chemosensitivity of AML cells through targeting FosB, Front. Med. 7 (2020) 582923, https://doi.org/10.3389/fmed.2020.582923.
[11] S. Tang, F. Zhang, J. Li, et al., The selective activator protein-1 inhibitor T-5224 regulates the IRF4/MYC axis and exerts cooperative antimyeloma activity with bortezomib, Chem. Biol. Interact. 384 (2023) 110687, https://doi.org/10.1016/j.cbi.2023.110687.
[12] J. Li, F. Cao, H.L. Yin, et al., Ferroptosis: past, present and future, Cell Death Dis. 11 (2) (2020) 88, https://doi.org/10.1038/s41419-020-2298-2.
[13] S.J. Dixon, K.M. Lemberg, M.R. Lamprecht, et al., Ferroptosis: an iron-dependent form of nonapoptotic cell death, Cell 149 (5) (2012) 1060–1072, https://doi.org/10.1016/j.cell.2012.03.042.
[14] D. Gao, R. Liu, Y. Lv, et al., A novel ferroptosis-related gene signature for predicting prognosis in multiple myeloma, Front. Oncol. 13 (2023) 999688, https://doi.org/10.3389/fonc.2023.999688.
[15] W.S. Yang, R. Sriramaratnam, M.E. Welsch, et al., Regulation of ferroptotic cancer cell death by GPX4, Cell 156 (1–2) (2014) 317–331, https://doi.org/10.1016/j.cell.2013.12.010.
[16] M. Dodson, R. Castro-Portuguez, D.D. Zhang, NRF2 plays a critical role in mitigating lipid peroxidation and ferroptosis, Redox Biol. 23 (2019) 101107, https://doi.org/10.1016/j.redox.2019.101107.

[17] K. Zeng, W. Li, Y. Wang, et al., Inhibition of CDK1 overcomes oxaliplatin resistance by regulating ACSL4-mediated ferroptosis in colorectal cancer, Adv. Sci. 10 (25) (2023) e2301088, https://doi.org/10.1002/advs.202301088.
[18] L. Zhao, X. Zhou, F. Xie, et al., Ferroptosis in cancer and cancer immunotherapy, Cancer Commun. 42 (2) (2022) 88–116, https://doi.org/10.1002/cac2.12250.
[19] W. Zhang, J. Dai, G. Hou, et al., SMURF2 predisposes cancer cell toward ferroptosis in GPX4-independent manners by promoting GSTP1 degradation, Mol. Cell 83 (23) (2023) 4352–4369, https://doi.org/10.1016/j.molcel.2023.10.042.
[20] Y. Zhong, F. Tian, H. Ma, et al., FTY720 induces ferroptosis and autophagy via PP2a/AMPK pathway in multiple myeloma cells, Life Sci. 260 (2020) 118077, https://doi.org/10.1016/j.lfs.2020.118077.
[21] W. Zhang, Q. Li, Y. Zhang, et al., Multiple myeloma with high expression of SLC7a11 is sensitive to erastin-induced ferroptosis, Apoptosis 29 (3–4) (2024) 412–423, https://doi.org/10.1007/s10495-023-01909-2.
[22] A.S. Alzahrani, PI3K/Akt/mTOR inhibitors in cancer: at the bench and bedside, Semin. Cancer Biol. 59 (2019) 125–132, https://doi.org/10.1016/j.semcancer.2019.07.009.
[23] Y. He, M.M. Sun, G.G. Zhang, et al., Targeting PI3K/Akt signal transduction for cancer therapy, Signal Transduct. Targeted Ther. 6 (1) (2021) 425, https://doi.org/10.1038/s41392-021-00828-5.
[24] M. Chi, J. Liu, C. Mei, et al., TEAD4 functions as a prognostic biomarker and triggers EMT via PI3K/AKT pathway in bladder cancer, J. Exp. Clin. Cancer Res. 41 (1) (2022) 175, https://doi.org/10.1186/s13046-022-02377-3.
[25] R. Dou, J. Qian, W. Wu, et al., Suppression of steroid 5alpha-reductase type I promotes cellular apoptosis and autophagy via PI3K/Akt/mTOR pathway in multiple myeloma, Cell Death Dis. 12 (2) (2021) 206, https://doi.org/10.1038/s41419-021-03510-4.
[26] Z. Yin, Y. Lv, L. Deng, et al., Targeting ABCB6 with nitidine chloride inhibits PI3K/AKT signaling pathway to promote ferroptosis in multiple myeloma, Free, Radic. Biol. Med. 203 (2023) 86–101, https://doi.org/10.1016/j.freeradbiomed.2023.04.003.
[27] J. Yi, J. Zhu, J. Wu, C.B. Thompson, X. Jiang, Oncogenic activation of PI3K-AKT-mTOR signaling suppresses ferroptosis via SREBP-mediated lipogenesis, Proc. Natl. Acad. Sci. U.S.A. 117 (49) (2020) 31189–31197, https://doi.org/10.1073/pnas.2017152117.
[28] F. Fan, P. Liu, R. Bao, et al., A dual PI3K/HDAC inhibitor induces immunogenic ferroptosis to potentiate cancer immune checkpoint therapy, Cancer Res. 81 (24) (2021) 6233–6245, https://doi.org/10.1158/0008-5472.CAN-21-1547.
[29] M.E. Ritchie, B. Phipson, D. Wu, et al., Limma powers differential expression analyses for RNA-sequencing and microarray studies, Nucleic Acids Res. 43 (7) (2015) e47, https://doi.org/10.1093/nar/gkv007.
[30] G. Yu, L.G. Wang, Y. Han, Q.Y. He, ClusterProfiler: an R package for comparing biological themes among gene clusters, OMICS 16 (5) (2012) 284–287, https://doi.org/10.1089/omi.2011.0118.
[31] A.J. Friedmann, M. Schneider, B. Proneth, et al., Inactivation of the ferroptosis regulator Gpx4 triggers acute renal failure in mice, Nat. Cell Biol. 16 (12) (2014) 1180–1191, https://doi.org/10.1038/ncb3064.
[32] L. Jiang, N. Kon, T. Li, et al., Ferroptosis as a p53-mediated activity during tumour suppression, Nature 520 (7545) (2015) 57–62, https://doi.org/10.1038/nature14344.
[33] A. Ruiz-Saenz, C. Dreyer, M.R. Campbell, V. Steri, N. Gulizia, M.M. Moasser, HER2 amplification in tumors activates PI3K/akt signaling independent of HER3, Cancer Res. 78 (13) (2018) 3645–3658, https://doi.org/10.1158/0008-5472.CAN-18-0430.
[34] K. Allmeroth, M. Horn, V. Kroef, S. Miethe, R.U. Muller, M.S. Denzel, Bortezomib resistance mutations in PSMB5 determine response to second-generation proteasome inhibitors in multiple myeloma, Leukemia 35 (3) (2021) 887–892, https://doi.org/10.1038/s41375-020-0989-4.
[35] Z. Wang, N. Shen, Z. Wang, et al., TRIM3 facilitates ferroptosis in non-small cell lung cancer through promoting SLC7a11/xCT K11-linked ubiquitination and degradation, Cell Death Differ. 31 (1) (2024) 53–64, https://doi.org/10.1038/s41418-023-01239-5.
[36] Y. Mou, J. Wang, J. Wu, et al., Ferroptosis, a new form of cell death: opportunities and challenges in cancer, J. Hematol. Oncol. 12 (1) (2019) 34, https://doi.org/10.1186/s13045-019-0720-y.
[37] X. Chen, R. Kang, G. Kroemer, D. Tang, Broadening horizons: the role of ferroptosis in cancer, Nat. Rev. Clin. Oncol. 18 (5) (2021) 280–296, https://doi.org/10.1038/s41571-020-00462-0.
[38] B. Hassannia, P. Vandenabeele, B.T. Vanden, Targeting ferroptosis to iron out cancer, Cancer Cell 35 (6) (2019) 830–849, https://doi.org/10.1016/j.ccell.2019.04.002.
[39] B.R. Stockwell, Ferroptosis turns 10: emerging mechanisms, physiological functions, and therapeutic applications, Cell 185 (14) (2022) 2401–2421, https://doi.org/10.1016/j.cell.2022.06.003.
[40] M.P. Murphy, H. Bayir, V. Belousov, et al., Guidelines for measuring reactive oxygen species and oxidative damage in cells and in vivo, Nat. Metab. 4 (6) (2022) 651–662, https://doi.org/10.1038/s42255-022-00591-z.
[41] K. Bersuker, J.M. Hendricks, Z. Li, et al., The CoQ oxidoreductase FSP1 acts parallel to GPX4 to inhibit ferroptosis, Nature 575 (7784) (2019) 688–692, https://doi.org/10.1038/s41586-019-1705-2.
[42] T. Steinbrunn, T. Stuhmer, C. Sayehli, M. Chatterjee, H. Einsele, R.C. Bargou, Combined targeting of MEK/MAPK and PI3K/Akt signalling in multiple myeloma, Br. J. Haematol. 159 (4) (2012) 430–440, https://doi.org/10.1111/bjh.12039.
[43] R. Tu, S. Wu, Z. Huang, et al., Neurotransmitter receptor HTR2B regulates lipid metabolism to inhibit ferroptosis in gastric cancer, Cancer Res. 83 (23) (2023) 3868–3885, https://doi.org/10.1158/0008-5472.CAN-23-1012.
[44] M. Merz, H. Salwender, M. Haenel, et al., Subcutaneous versus intravenous bortezomib in two different induction therapies for newly diagnosed multiple myeloma: an interim analysis from the prospective GMMG-MM5 trial, Haematologica 100 (7) (2015) 964–969, https://doi.org/10.3324/haematol.2015.124347.
[45] L. Cao, H. Gu, Z. Zhang, E. Zhang, J. Chang, Z. Cai, Calcium silicate/bortezomib combinatory therapy for multiple myeloma, Journal of materials chemistry. B, Materials for biology and medicine 11 (9) (2023) 1929–1939, https://doi.org/10.1039/d2tb02009b.
[46] R. Xu, Y. Li, H. Yan, et al., CCL2 promotes macrophages-associated chemoresistance via MCPIP1 dual catalytic activities in multiple myeloma, Cell Death Dis. 10 (10) (2019) 781, https://doi.org/10.1038/s41419-019-2012-4.